Evolution Conserves the Network of Coupled Residues in Dihydrofolate Reductase

Author List: Jiayue Li,[1] Gabriel Fortunato,[1] Jennifer Lin,[1] Pratul K. Agarwal,[2] Amnon Kohen,[1] Priyanka Singh,*[1] Christopher M. Cheatum*[1]

Institution Addresses:

[1] Department of Chemistry, University of Iowa, Iowa City, IA 52242

[2]Department of Biochemistry & Cellular and Molecular Biology, University of Tennessee, Knoxville, TN 37996

Author Information Notes:

* Authors to whom correspondences should be addressed:

E-mail: priyankanarendra-singh@uiowa.edu Phone: +1 319 621 8572

Email: christopher-cheatum@uiowa.edu Phone: +1 319 621 2980

ABSTRACT

Understanding protein motions and their role in enzymatic reactions is an important and timely topic in enzymology. Protein motions that are involved in the chemical step of catalysis are particularly intriguing but difficult to identify. A global network of coupled residues in *Escherichia coli* dihydrofolate reductase (*E. coli* DHFR), which assists in catalyzing the chemical step, has previously been demonstrated through quantum mechanical/molecular mechanical and molecular dynamics simulations, as well as bioinformatic analyses. A few specific residues — M42, G121, F125 and I14 — were shown to function synergistically with measurements of single turnover rates and the temperature dependence of intrinsic kinetic isotope effects ($KIEs_{int}$) of site directed mutants. The current study hypothesizes that the global network of residues involved in the chemical step is evolutionarily conserved and probes homologous residues of the potential global network in human DHFR through measurements of the temperature dependence of $KIEs_{int}$ and computer simulations based on empirical valence bond (EVB) method. We study the mutants M53W and S145V. Both of these remote residues are homologous to network residues in *E. coli* DHFR. Non-additive isotope effects on activation energy are observed between M53 and S145, indicating their synergistic effect on the chemical step in human DHFR, which suggests that both of these residues are part of a network affecting the chemical step in enzyme catalysis. This finding supports the hypothesis that human and *E. coli* DHFR share similar networks, consistent with evolutionary preservation of such networks.

INTRODUCTION

Dihydrofolate reductase (DHFR) is a paradigmatic enzyme for protein dynamics studies.[1-15] It is a ubiquitous enzyme that catalyzes the reduction of 7,8-dihydrofolate (DHF) to 5,6,7,8-tetrahydrofolate (THF) by stereospecific hydride transfer from the pro-4R position of NADPH to the C6 position of the pterin ring of DHF. DHFR plays an important role in the maintenance of cellular THF levels and is essential for the biosynthesis of pyrimidine nucleotides and amino acids. Structural information obtained by X-ray diffraction and NMR relaxation dispersion has shown that three distinct enzyme conformations exist along the catalytic pathway of *E. coli* DHFR: open, closed, and occluded.[16] NMR dispersion relaxation experiments show that the bonding of both substrate and cofactor induces a conformational change in the M20 loop (residues 9-24), as well as other conformational changes that are not restricted to the active site.[17-19] QM/MM/MD studies[20-22] and bioinformatics investigations[23] have identified a network of coupled residues whose motions correlate with the chemical step in *E. coli* DHFR. Experimental approaches have substantiated the existence of this network including transient kinetics,[24] the temperature dependence of intrinsic kinetic isotope effects ($KIEs_{int}$),[10, 25] and NMR relaxation.[26] One of the interesting features of this

network is the conservation of not only active-site residues like I14, but also distal ones like M42, G121, and F125. Indeed, structural and computational analyses have provided evidence that the motions of conserved distal residues affect the catalyzed reactions for *E. coli* DHFR as well as cyclophilin A (CypA).[27] QM/MM computational analysis of *Bacillus subtilis* DHFR have found a similar network facilitating the hydride transfer step, as this enzyme contains a residue equivalent to *E. coli*'s M42.[28] In contrast, QM/MM studies by transition path sampling suggested that protein promoting vibrations are coupled to the hydride transfer step for human DHFR but not for ecDHFR,[3, 29] though these promoting vibrations differ in many respects from the networks of coupled residues.[30] Thus, it is still not clear whether either promoting vibrations or networks of coupled residues are absent or present for enzymes in general, or if *E. coli* DHFR is a special case. Further explorations of human DHFR could help us understand if and to what extent the network in *E. coli* DHFR is preserved through evolution. The presence of a network of coupled residues has been reported to be important in an increasing number of enzyme systems, however, an ongoing concern has been whether these networks play an active role in enzyme function or if observed coupled motions are merely a coincident effect of the rearrangement of atoms/residues

as a result of catalysis. Even though direct evidence supporting the role of these networks as a promoting factor in catalysis remains elusive, information obtained from a variety of experimental and computational investigations suggests that these networks are a conserved part of enzyme folds[27] and play active-roles in catalysis. Mutation of distal network residues[20, 31, 32] and modulation of enzyme dynamics using miscible organic solvents[33] has been shown to decrease the enzyme rate, while engineered protein constructs have been used to relay allosteric signals that these pathways initiated by photo-activation.[34] The collective evidence suggests that these protein motions and networks play an active role in enzyme mechanisms. Further investigations are still required to characterize whether the motions in these networks are *caused due to* or *affect* catalysis.

Human DHFR shares a 27% primary sequence identity with *E. coli* DHFR (**Figure S1**). Unlike in bacterial enzymes, the M20 loop of human DHFR remains only in the closed conformation, as indicated by both binary and ternary complex crystal structures.[35, 36] NMR studies have demonstrated that human DHFR requires minimal side chain rearrangements through its catalytic cycle, with only the adenosine-binding subdomain undergoing rearrangement.[37] Despite these differences, human DHFR catalyzes the same reaction as its *E. coli* ortholog with similar catalytic

turnover rates. The two enzymes share a common structural scaffold, as displayed in **Figure 1**. [38, 39] Therefore, we hypothesize that human DHFR preserves a similar network of coupled residues modulating hydride transfer. In complex enzymatic reactions that involve many steps, it is challenging to isolate the chemical step. Here, we take advantage of the temperature dependence of intrinsic kinetic isotope effect (KIEs) measurements to achieve that isolation.

Kinetic isotope effect (KIE) measurements have been used for many enzymatic studies, especially in explaining C-H bond activation. Intrinsic KIEs ($KIEs_{int}$) isolate the chemical step from the complicated enzymatic kinetic cascade. The temperature dependence of $KIEs_{int}$ is a well-established way of studying the sampling of the donor-acceptor distance (DAD) distribution for hydrogen transfer reaction, the interpretation of which is based on a phenomenological model known as the "Activated Tunneling Model". [40] As is discussed previously[41, 42], the DAD sampling is assumed to be an equilibrium property of the system. A majority of wild-type enzymes exhibit temperature independent $KIEs_{int}$, which are readily explained by this phenomenological model.[43, 44] Although formally only appropriate to non-adiabatic hydrogen transfer reactions, the basic phenomenology of the activated tunneling model serves a suitable qualitative picture for

interpreting the temperature dependence of primary kinetic isotope effects even for adiabatic hydrogen transfer reactions.[40, 45] According to the activated tunneling model, if the DAD distribution at the tunneling ready state (TRS) is narrow, then there is very little effect of temperature on the DAD. As a result, the temperature has negligible effect on the tunneling probability, giving rise to a temperature independent KIE across the narrow range of temperatures that is accessible for folded proteins. In contrast, mutations that broaden the DAD distribution lead to temperature dependent KIEs as a result of the thermally activated sampling of the DAD distribution that modulates the tunneling probability.[15, 41, 46] The temperature dependence of $KIEs_{int}$ is, therefore, a powerful technique for characterizing the distribution of DADs, the distance between C4 of NADPH and C6 of DHF in the case of DHFR, at the TRS for the catalyzed reaction within the phenomenological framework of the activated tunneling model.[5, 40]

We explore evolutionary conservation of the network of coupled residues in DHFR, both experimentally and theoretically. The analogs to the highly conserved residues M42 and G121 of *E. coli* are identified in human DHFR through sequence alignment (**Figure S1**). In addition to the single mutants M53W and S145V, we also study the double mutant, M53W-S145V, (see **Figure 1**)

to probe for synergistic effects. Steady state kinetic measurements for M53W, S145V, and M53W-S145V human DHFR variants assess whether mutations of these distal residues significantly lessen overall catalytic efficiency and turnover. Because these experiments do not provide direct information on the chemical step, we employ the temperature dependence of $KIEs_{int}$ to probe the DAD sampling involved in the hydride transfer. Further, we use computational simulations of hydride transfer to investigate the behavior of network residues and correlated motions for all three mutants, as well as for wild-type human and *E. coli* enzymes. Results show that the conserved residues M53 and S145 are both part of a network of correlated residues that affect the hydride transfer in the human enzyme. This finding supports the hypothesis that the global network of coupled residues is conserved in the evolution from *E. coli* to human DHFR.

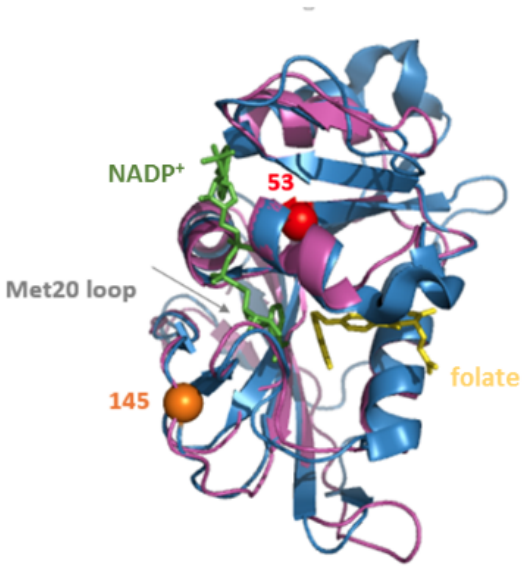

Figure 1. Superposition of human (blue; PDB ID 4M6K) and *E. coli* DHFR (pink; PDB ID 1RX2) bound to $NADP^+$ and folate. The ligands are shown as green (NADPH) and yellow (DHF) sticks; human DHFR residues M53 (red) and S145 (orange) are shown as spheres.

EXPERIMENTAL METHODS

All human DHFR mutants are generated through site-directed mutagenesis and purified with modifications as described in the SI. Competitive measurements of the temperature dependence of intrinsic KIEs were carried out by conducting H/T and D/T measurements, and intrinsic value can be accessed with Northrop Method as described previously[5, 47]. Detailed methodology is described in the SI.

Computational Modeling of Hydride Transfer

For modeling the hydride transfer step, we use a protonated substrate (DHF^+) and the EVB method developed by Warshel and coworkers,[48, 49] as implemented in AMBER (v14). The modeled enzymatic reaction is the hydride transfer from NADPH (cofactor) to protonated DHF to produce $NADP^+$ and THF. The starting structure for the enzyme is based on structure 4M6K from the Protein Data Bank. EVB sampling aggregates 95 ns for wild-type and the 3 mutant systems. Analyses of the geometrical quantities and correlations are performed as previously reported[22, 27]. See the SI for more details.

RESULTS AND DISCUSSION

Experimental evidence for the network of coupled motions in human DHFR

We measure competitive KIEs on the second-order rate constant k_{cat}/K_M for each mutant and the wild-type human DHFR. $KIEs_{int}$ are fit to the Arrhenius equation as previously described[10, 25, 31, 43, 44, 46] to obtain isotope effects on the activation energy ($\Delta E_{a(T-H)} = (\Delta Ea_T - (\Delta Ea_H)$ as well as on Arrhenius pre-exponential factors (A_H/A_T), in which H and T indicate protium and tritium isotopologues, respectively. **Table 1** summarizes the results of these measurements, and **Figure 2** shows the Arrhenius plots of the human wild-type enzyme and mutants M53W, S145V, and M53W-S145V (right) along with the equivalent *E. coli* enzymes (left) as measured previously,[50] namely M42W, G121V, and M42W-G121V.[26] **Table S1** reports the observed and intrinsic KIEs (with standard deviations) for all human mutants, and **Figures S2-4** show the corresponding Arrhenius plots.

	***E. coli* DHFR[a]**				**Human DHFR**			
	WT	**M42W**	**G121V**	**M42W-G121V**	**WT**	**M53W**	**S145V**	**M53W-S145V**
A_H/A_T	7.0 ± 1.5	2.8 ± 0.2	7.4 ± 1.6	0.011 ± 0.004	6.6 ± 0.8	1.5 ± 0.2	1.4 ± 0.2	0.030 ± 0.008
$\Delta E_{a(T-H)}$ kcal/mol	-0.1± 0.2	0.58 ± 0.04	0.23 ± 0.03	3.6 ± 0.3	-0.1± 0.1	1.03 ± 0.06	0.7 ± 0.1	3.7 ± 0.1

$\Delta\Delta E_{a(T\text{-}H)}$ kcal/mol	2.8 ± 0.3	2.0 ± 0.2

Table 1. Comparative isotope effects for human and *E. coli* DHFR mutants at pH 9.0. [a] ref.43
$\Delta\Delta E_{a(T\text{-}H)} = \Delta E_{a(T\text{-}H)\ mutant1\text{-}2} - (\Delta E_{a(T\text{-}H)\ mutant1} + \Delta E_{a(T\text{-}H)\ mutant2})$.

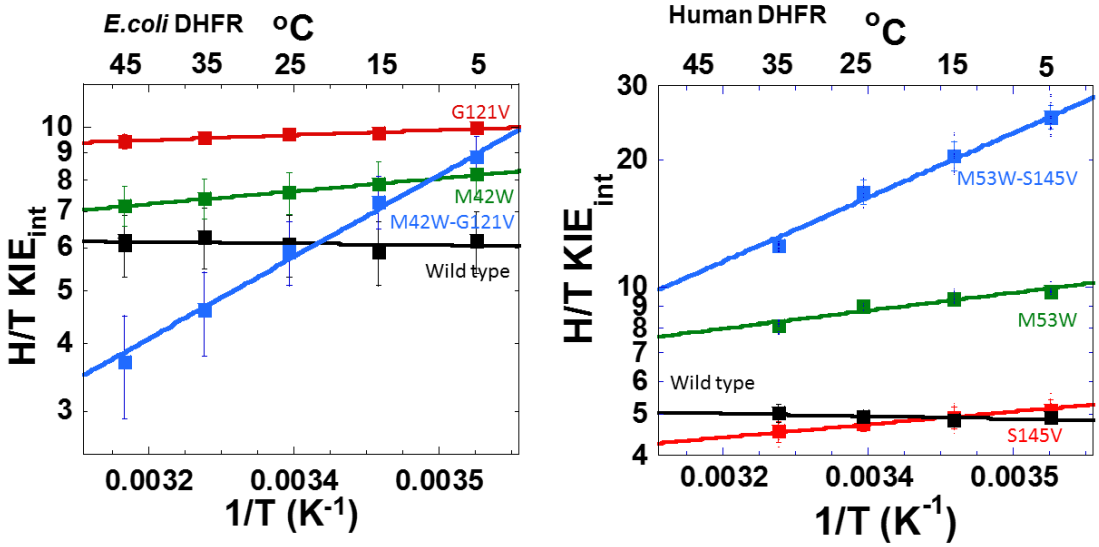

Figure 2. Arrhenius plots of intrinsic H/T KIEs for wild-type human DHFR and mutants (left), as well as wild-type *E. coli* DHFR and analogous mutants (right). Wild-type enzymes are shown in black,[44] M53W (human) and M42W (*E. coli*) green, S145V (human) and G121V (*E. coli*) red, and M53W-S145V (human) and M42W-G121V (*E. coli*)[50] blue.

As indicated in **Figure 2**, each of the single mutants of human DHFR shows similar KIE behavior to the corresponding *E. coli* mutant, i.e. slightly temperature-dependent $KIEs_{int}$. Within the framework of to the activated-tunneling model, these results suggest that the single mutants sample broader DAD ensembles at the TRS and have less organized reactive states than the optimized wild type enzyme. For the double mutant M53W-S145V, we observe a steep temperature dependence of the isotope effect, $\Delta E_{a(T\text{-}H)}$, much larger than 1 kcal/mol, as well as

inflated KIEs relative to single mutants as shown in **Table 1**. The isotope effect on the activation energy of the double mutant is much larger than the sum of the values for the two single mutants ($\Delta E_{a(T\text{-}H)M53W\text{-}S145V} > \Delta E_{a(T\text{-}H)M53W} + \Delta E_{a(T\text{-}H)S14V}$). This non-additivity indicates a synergistic effect between residues M53 and S145, which is indicative coupling between the involved residues. Thus, despite both residues being distal, the effects of the two residues are coupled, giving rise to the nonadditive influence on the catalyzed hydride transfer reaction in human DHFR and suggesting that a similar network to the one that has been mapped out in *E. coli* DHFR exists in human DHFR.

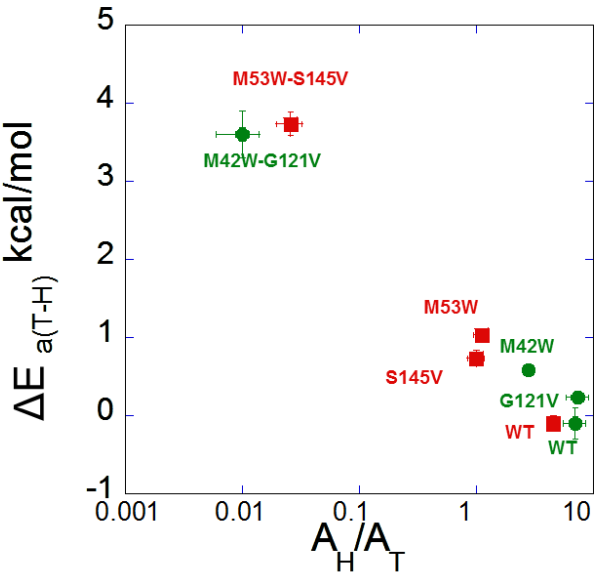

Figure 3. Correlation of temperature dependence parameters (isotope effect on activation energy and pre-exponential factor ratio) for human DHFR mutants M53W, S145V, M53W-S145V, and wild type (red squares), as well as *E. coli* DHFR mutants M42W, G121V, M42W-G121V, and wild type (green circles).

Figure 3 shows the correlation between the isotope effect on activation energy ($\Delta E_{a(T-H)}$) and the pre-exponential factor ratio (A_H/A_T), for both human mutants (red squares) and their corresponding *E. coli* mutants (green circles). The human single mutants (M53W and S145V) are clustered around the same region as the *E. coli* single mutants (M42W and G121V). This region involves larger A_H/A_T values, but small changes in isotope effect on the activation energy. The human double mutant (M53W-S145V) is more similar to its *E. coli* analogue (M42W-G121V). Each has steeply temperature-dependent KIE_{int} and a small isotope effect on the pre-exponential factors. For both the *E. coli* and human double mutants, the magnitude of $\Delta E_{a(T-H)}$ is larger than the sum of $\Delta E_{a(T-H)}$ values for the single mutants indicating that the remote residues are synergistically involved in the hydride transfer. This feature emphasizes the similarity between the networks assisting hydride transfer in both human DHFR and *E. coli* DHFR.

Computational simulations of hydride transfer by wild-type human DHFR and mutants

We use computational simulations based on the empirical valence bond (EVB) method to explore the role of distal residues in the protein network and their effects on the hydride-transfer

step. This approach has been used previously to explore conformational dynamics associated with hydride transfer for *E. coli* DHFR and several of its mutants. Past *E. coli* results indicated that several residues, including I14, G15, F31, M42, Y100, G121, and D122, form a coupled network that promotes bond cleavage.[22, 51] Motions starting from the surface region and mediated by other residues induce changes in the active-site geometry that bring the donor and acceptor atoms toward each other and facilitate the reaction.

The *E. coli* network was proposed to modulate the active site by two mechanisms. In one, motions start from the surface with D122 and are relayed through hydrogen bonding between pairs of residues: D122-G15 and I14-Y100. Y100 induces puckering motions of the NADPH ring, which contains the donor carbon, C_D. In the other mechanism, F31 induces puckering of the pterin ring of DHF^+, which mediates the angle of the DHF^+ tail (C_A-C_9-N_{10}).

Figures 4 and **5** show the computational results for wild-type and mutants of human DHFR. The behavior of the proposed network residues in human DHFR is similar to the previously reported behavior of corresponding *E. coli* residues. The DADs show identical profiles as a function of the reaction coordinate for the wild-type enzymes of both species, as well as all

mutants investigated in this study (**Figure 4A**). The observed behavior of DADs is identical to previously reported studies of *E. coli* DHFR, human DHFR, and N23PP and N23PP/G51PEKN mutants of *E. coli* DHFR.[52] In this previous study, the DAD was also seen to decrease from ~3.5 Å to below 2.8 Å as the reaction approached transition state, and then increased to over 3.4 Å in the product state. The impact of the motions on the hybridization states (**Figure 4B**) of C_D (donor) and C_A (acceptor) is also similar for wild-type human and *E. coli* DHFR, but with minor differences for the DHF^+ ring.

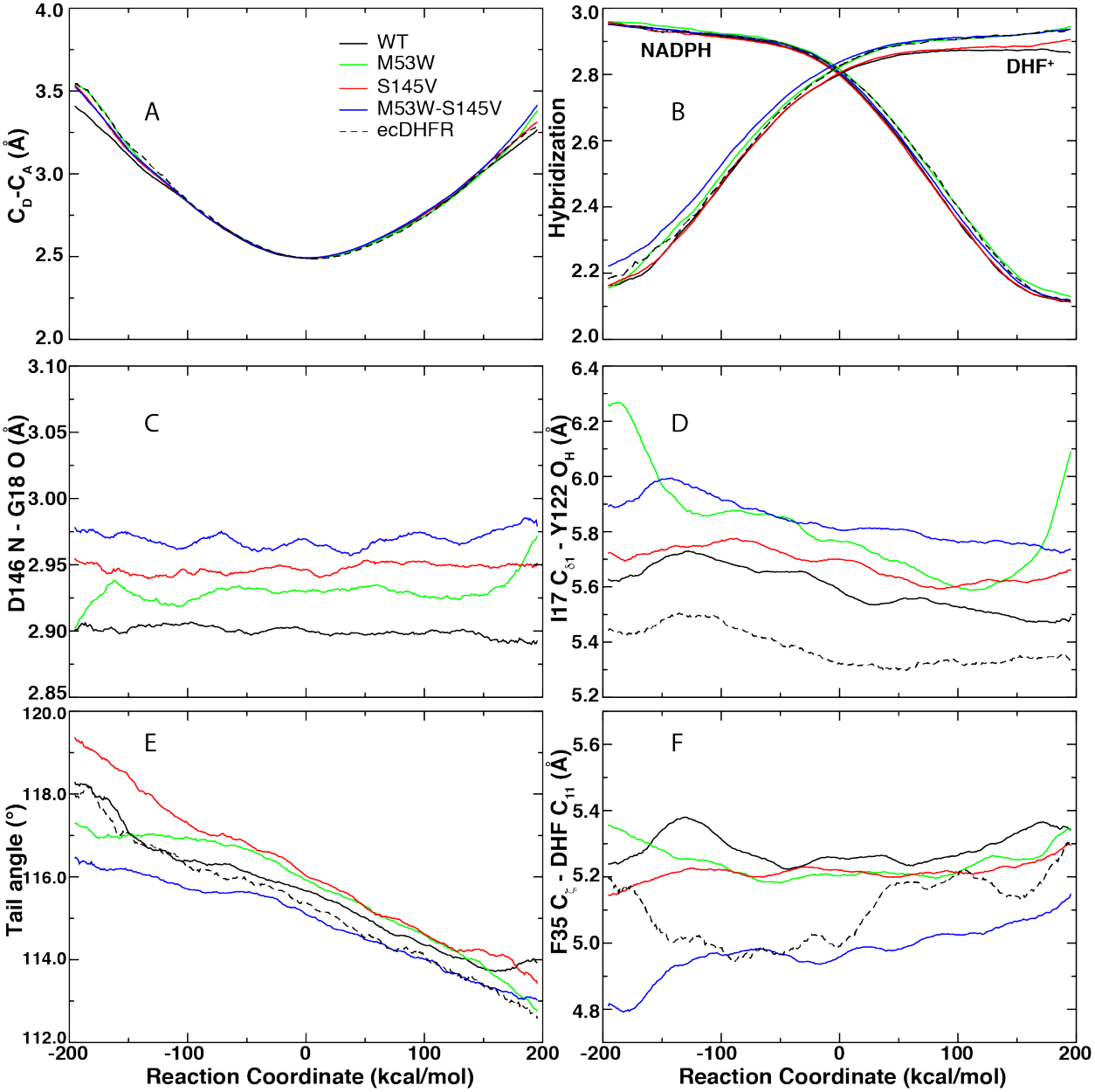

Figure 4: Behavior of network residues (numbered according to human DHFR numbering) for wild-type human (solid black line) and *E. coli* DHFR (dashed black line), as well as human mutants (colored lines). **A)** C_D (donor carbon)-C_A (acceptor carbon) distances; **B)** States of hybridization at C_D (NADPH) and C_A (DHF^+); **C)** Distances between the N atom of D146 and the O atom of G18, which interact via hydrogen bonding; **D)** I17 $C_{\delta 1}$ – Y122 O_H distance; **E)** DHF tail angles; **F)** F35 C_ζ - DHF C_{11} distance. These network geometrical parameters are equivalent to the ones defined in Ref[22] for *E. coli* DHFR. In panel **C)**, the *E. coli* DHFR H-bond is not shown, as in the current simulation it is over 5 Å. However, the distance has been shown elsewhere to be close to the human DHFR values reported here.

The mutations of the human enzyme perturb how the network regulates C_D, as residues M53 and S145 are both associated with changes in the puckering of the NADPH ring. Therefore, the D146-G18 hydrogen bond (equivalent to the D122-G15 hydrogen bond in *E. coli* DHFR) is weakened for both single mutants and the double mutant (**Figure 4C**). This effect is then relayed to the active site through an increase in the distance between I17 and Y122 (corresponding to I14 and Y100 from the *E. coli* enzyme) (**Figure 4D**), which is consistent with the empirically observed decrease in turnover number. Note that in **Figure 4C**, the H-bond distance for *E. coli* is not shown in the panel, as it is more than 5 Å in our simulations. This is likely a limitation of the starting conformation, however the importance of this network interaction has been confirmed in several other studies. [27,31,50]

F35 (equivalent to F31 in *E. coli* DHFR) has been proposed to induce puckering of the pterin ring of DHF^+, which mediates the angle of the DHF^+ tail containing C_A. The behavior of this residue does not show consistent changes with the mutations, as the decrease in tail angle occurs in wild-type human and *E. coli* DHFR as well as all three human mutants (**Figure 4E**). The distance between F35 and DHF^+ is similar for the single mutants and wild type. For the double

mutant, there is an overall shift in the F35-DHF^{+} distance, and this effect is likely due to active-site rearrangements that compensate for the effects of the mutations. Mutations of F35 and/or nearby residues would be required to confirm the role of this reside in the network. Overall, the behavior of network residues is similar in the cases of human and *E. coli* DHFR.

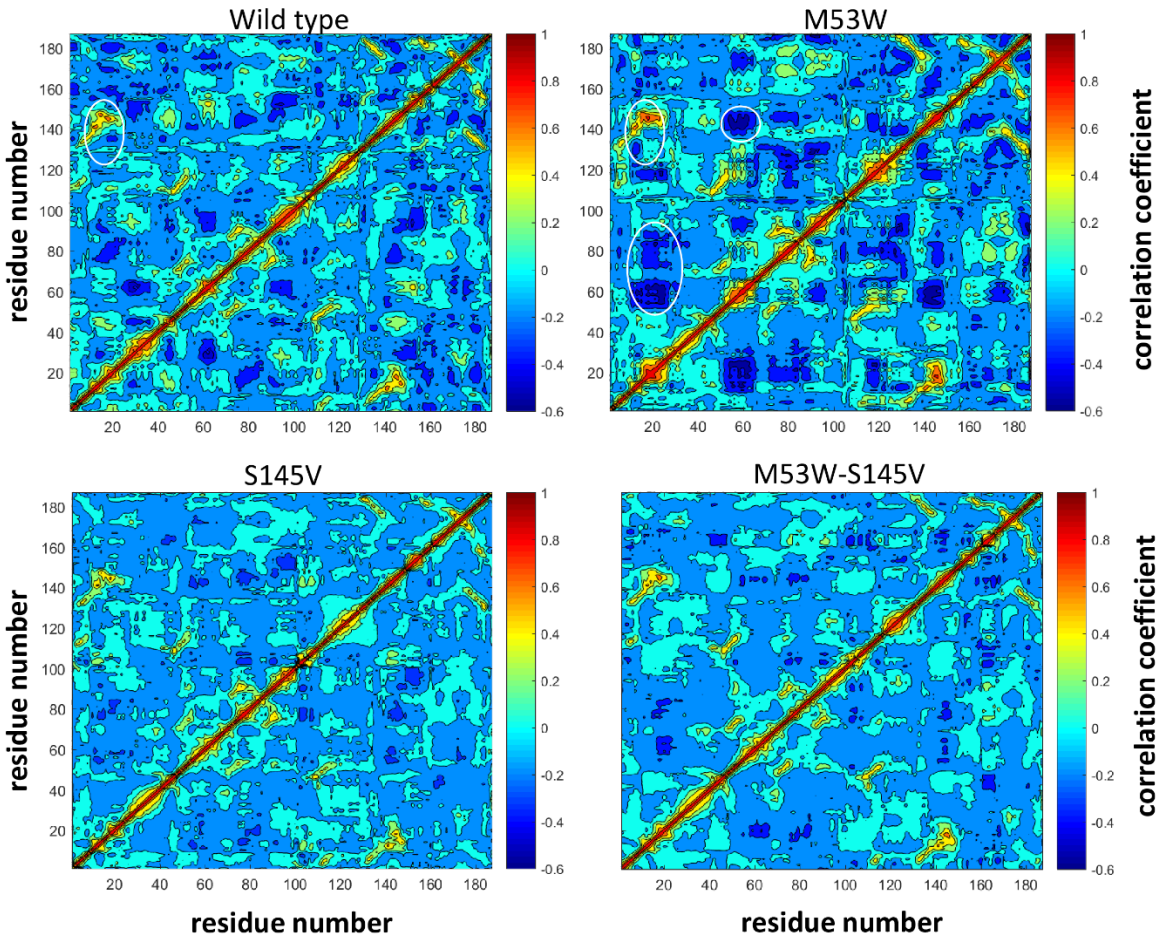

Figure 5: Dynamic cross-correlation for wild-type human DHFR and mutants. The correlation shows significant changes, which are marked with white ellipses.

Figure 5 shows correlation maps of the enzyme motions for the wild-type and mutant enzymes. Compared to the wild-type human enzyme, the M53W mutant shows significant

changes in the correlations of the M20 loop with residues 130-145, as well as additional regions (marked with white ellipses in the Figure). Also, a significant increase in negative correlations (dark blue regions in the plot) is observed in some regions for the M53W mutant. However, for both S145V and the double mutant, the off-diagonal areas of both positive and negative correlation show smaller magnitudes compared to the wild type. The plots indicate that these distal mutations affect the correlations of the entire enzyme. In combination with experimental data and the analysis of network residues (**Figure 4**), the overall results indicate that the investigated residues participate in a network similar to the one reported for *E. coli* DHFR.[22] Note that these maps report on the overall correlated motions observed in the protein and do not isolate functionally relevant motions. Further detailed study would be required to obtain quantitative comparison of the functionally relevant motions of the network residues and their effects on the rate of hydride transfer.

The similarities or differences between human and *E. coli* DHFRs have been the subject of some disagreement in the literature. A recent computational study from Schwartz and coworkers, based on committor calculations and kernel principal component analysis, indicated that I17 and

F35 are closely packed and their fast motions (picosecond time-scale) couple to the reaction coordinate of hydride transfer reaction as part of a promoting vibration in the human enzyme that is not present in the *E. coli* enzyme.[29] Such promoting vibrations, however, are distinct from the networks of residues that we identify here. The promoting vibrations that have been reported for the human enzyme based on computational studies from the Schwartz group are described as "nonequilibrium density fluctuations" of the protein. In contrast, the motions of the network of coupled residues that we report and that have been previously identified for the *E. coli* enzyme involve equilibrium motions of the protein. Thus, although some previous studies, both computational and using isotopically heavy enzymes, indicate that there may be differences between human and *E. coli* DHFRs,[29, 53] our results show that the network of residues that are involved in organizing the active site for efficient hydride transfer in the *E. coli* enzyme is preserved in the human enzyme. Our previous studies of the protein mass modulation effects in these enzymes showed that isotopically labelling the protein can cause perturbations to the protein structure and stability that go beyond what is expected as a result of a mass alteration alone.[12, 44] The complications associated with interpreting the effects of isotopic substitution of

the whole protein on both the mass and the electrostatics of the enzyme raise some concern about the interpretation of the reported differences between *E. coli* and human DHFRs based on such studies. In contrast, we suggest that the current study offers strong evidence in support of the evolutionary preservation of the network of coupled residues involved in the catalyzed hydride transfer from *E. coli* to human enzymes. Clearly, reconciling these differing conclusions will require further study.

CONCLUSION

Explorations of protein motions are of great interest for their potential benefit in understanding enzyme catalysis, including work on networks of coupled residues involving long-range effects of remote residues on the chemical step. Our work explores the conservation of these networks through evolution. Two equivalent and conserved distal residues from a well-established *E. coli* network are identified and studied here for human DHFR, namely M53W and S145V, and the double mutant (M53W-S145V). Synergistic behavior between the residues is observed from the temperature dependence of KIE studies, reinforcing the notion that both residues are coupled to each other in their effect on the hydride transfer. Further, computational modeling of the mutants

and the wild type also indicates that the residues M53 and S145 participate in a network that resembles the one reported for *E. coli* DHFR. Particularly, these residues play a role in the side of the network that starts from surface βF-βG and the M20 loop, and is later relayed through Y122 to pucker the NADPH ring and modulate the position of the donor carbon (C_D). Mutations of these residues change the correlations of motions throughout the entire enzyme. Again, this finding mirrors the case reported for *E. coli* DHFR.

Together, the experimental and computational results show that despite low sequence identity and differences in some conformational rearrangements between the two enzymes, the network of coupled residues in DHFR has been preserved along the evolutionary line from *E. coli* to humans. We have shown that a network of residues that facilitates the chemical step, exists in both human and bacterial enzymes. Further studies could be focused on generalizing the existence of such networks in enzyme catalysis. Rational drug design and creative design of homologous enzymes by protein engineering could benefit from understanding coupled networks that influence the chemical step.

ACCESSION CODES

DYR_HUMAN P00374

DYR_ECOLI P0ABQ4

ACKNOWLEDGEMENTS

The authors gratefully acknowledge funding for this work from the National Science Foundation under grant CHE-1707598 (CMC).

Supporting Information: Includes details of the experimental and computational approach including materials, methods, preparation of human DHFR, competitive intrinsic KIE measurements and kinetic complexity calculations, computational modeling of hydride transfer, equilibrium geometrical properties, and associated supplementary figures and tables.

REFERENCES

[1] Arora, K., and Brooks III, C. L. (2009) Functionally Important Conformations of the Met20 Loop in Dihydrofolate Reductase are Populated by Rapid Thermal Fluctuations, *J. Am. Chem. Soc. 131*, 5642-5647.

[2] Bystroff, C., and Kraut, J. (1991) Crystal structure of unliganded Escherichia coli dihydrofolate reductase. Ligand-induced conformational changes and cooperativity in binding, *Biochemistry 30*, 2227-2239.

[3] Dametto, M., Antoniou, D., and Schwartz, S. D. (2012) Barrier Crossing in Dihydrofolate Reductasedoes not involve a rate-promoting vibration, *Mol Phys 110*, 531-536.

[4] Fierke, C. A., Johnson, K. A., and Benkovic, S. J. (1987) Construction and evaluation of the kinetic scheme associated with dihydrofolate reductase from Escherichia coli, *Biochemistry 26*, 4085-4092.

[5] Klinman, J. P., and Kohen, A. (2013) Hydrogen tunneling links protein dynamics to enzyme catalysis, *Annu. Rev. Biochem. 82*, 471-496.

[6] Liu, H., and Warshel, A. (2007) The Catalytic Effect of Dihydrofolate Reductase and Its Mutants Is Determined by Reorganization Energies†, *Biochemistry 46*, 6011-6025.

[7] Loveridge, E. J., Behiry, E. M., Guo, J., and Allemann, R. K. (2012) Evidence that a 'dynamic knockout' in Escherichia coli dihydrofolate reductase does not affect the chemical step of catalysis, *Nat. Chem. 4*, 292-297.

[8] McElheny, D., Schnell, J. R., Lansing, J. C., Dyson, H. J., and Wright, P. E. (2005) Defining the role of active-site loop fluctuations in dihydrofolate reductase catalysis, *Proceedings of the National Academy of Sciences of the United States of America 102*, 5032-5037.

[9] Pauling, L. (1948) Chemical Achievement and Hope for the Future, *Am. Sci. 36*, 51-58.

[10] Singh, P., Francis, K., and Kohen, A. (2015) Network of Remote and Local Protein Dynamics in Dihydrofolate Reductase Catalysis, *ACS Catalysis 5*, 3067-3073.

[11] Singh, P., Morris, H., Tivanski, A. V., and Kohen, A. (2015) A calibration curve for immobilized dihydrofolate reductase activity assay, *Data in Brief 4*, 19-21.

[12] Wang, Z., Singh, P., Czekster, C. M., Kohen, A., and Schramm, V. L. (2014) Protein Mass-Modulated Effects in the Catalytic Mechanism of Dihydrofolate Reductase: Beyond Promoting Vibrations, *J. Am. Chem. Soc. 136*, 8333-8341.

[13] Wong, K. F., Watney, J. B., and Hammes-Schiffer, S. (2004) Analysis of Electrostatics and Correlated Motions for Hydride Transfer in Dihydrofolate Reductase, *J. Phys. Chem. B 108*, 12231-12241.

[14] Nagel, Z. D., and Klinman, J. P. (2010) Update 1 of: Tunneling and Dynamics in Enzymatic Hydride Transfer, *Chem. Rev. 110*, PR41-PR67.

[15] Klinman, J. P., and Offenbacher, A. R. (2018) Understanding Biological Hydrogen Transfer Through the Lens of Temperature Dependent Kinetic Isotope Effects, *Accounts of Chemical Research 51*, 1966-1974.

[16] Sawaya, M. R., and Kraut, J. (1997) Loop and subdomain movements in the mechanism of Escherichia coli dihydrofolate reductase: crystallographic evidence, *Biochemistry 36*, 586-603.

[17] McElheny, D., Schnell, J. R., Lansing, J. C., Dyson, H. J., and Wright, P. E. (2005) Defining the role of active-site loop fluctuations in dihydrofolate reductase catalysis, *Proc. Natl. Acad. Sci. U.S.A. 102*, 5032-5037.

[18] Venkitakrishnan, R. P., Zaborowski, E., McElheny, D., Benkovic, S. J., Dyson, H. J., and Wright, P. E. (2004) Conformational Changes in the Active Site Loops of Dihydrofolate Reductase during the Catalytic Cycle, *Biochemistry 43*, 16046-16055.

[19] Osborne, M. J., Schnell, J., Benkovic, S. J., Dyson, H. J., and Wright, P. E. (2001) Backbone Dynamics in Dihydrofolate Reductase Complexes: Role of Loop Flexibility in the Catalytic Mechanism, *Biochemistry 40*, 9846-9859.

[20] Wong, K. F., Selzer, T., Benkovic, S. J., and Hammes-Schiffer, S. (2005) Impact of distal mutations on the network of coupled motions correlated to hydride transfer in dihydrofolate reductase, *Proc. Natl. Acad. Sci. U.S.A. 102*, 6807-6812.

[21] Radkiewicz, J. L., and Brooks, C. L. (2000) Protein Dynamics in Enzymatic Catalysis: Exploration of Dihydrofolate Reductase, *J. Am. Chem. Soc. 122*, 255-231.

[22] Agarwal, P. K., Billeter, S. R., Rajagopalan, P. T., Benkovic, S. J., and Hammes-Schiffer, S. (2002) Network of coupled promoting motions in enzyme catalysis, *Proc. Natl. Acad. Sci. U.S.A. 99*, 2794-2799.

[23] Hammes-Schiffer, S., and Benkovic, S. J. (2006) Relating protein motion to catalysis, *Annu. Rev. Biochem. 75*, 519-541.

[24] Rajagopalan, P. T. R., Stefan, L., and Benkovic, S. J. (2002) Coupling Interactions of Distal Residues Enhance Dihydrofolate Reductase Catalysis: Mutaional Effects on Hydride Transfer Rates, *Biochemistry 41*, 12618-12628.

[25] Singh, P., Sen, A., Francis, K., and Kohen, A. (2014) Extension and Limits of the Network of Coupled Motions Correlated to Hydride Transfer in Dihydrofolate Reductase, *J. Am. Chem. Soc. 136*, 2575-2582.

[26] Boehr, D. D., Schnell, J. R., McElheny, D., Bae, S.-H., Duggan, B. M., Benkovic, S. J., Dyson, H. J., and Wright, P. E. (2013) A Distal Mutation Perturbs Dynamic Amino Acid Networks in Dihydrofolate Reductase, *Biochemistry 52*, 4605-4619.

[27] Ramanathan, A., and Agarwal, P. K. (2011) Evolutionarily Conserved Linkage between Enzyme Fold, Flexibility, and Catalysis, *PLOS Biology 9*, e1001193.

[28] Hammes-Schiffer, S., and Watney, J. B. (2006) Hydride transfer catalysed by Escherichia coli and Bacillus subtilis dihydrofolate reductase: coupled motions and distal mutations, *Philos. Trans. R. Soc. B 361*, 1365-1373.

[29] Masterson, J. E., and Schwartz, S. D. (2015) Evolution Alters the Enzymatic Reaction Coordinate of Dihydrofolate Reductase, *The Journal of Physical Chemistry. B 119*, 989-996.

[30] Kohen, A. (2015) Role of Dynamics in Enzyme Catalysis: Substantial versus Semantic Controversies, *Accounts of Chemical Research 48*, 466-473.

[31] Wang, L., Tharp, S., Selzer, T., Benkovic, S. J., and Kohen, A. (2006) Effects of a distal mutation on active site chemistry, *Biochemistry 45*, 1383-1392.

[32] Wang, L., Goodey, N. M., Benkovic, S. J., and Kohen, A. (2006) The role of enzyme dynamics and tunnelling in catalysing hydride transfer: studies of distal mutants of dihydrofolate reductase, *Philos. Trans. R. Soc. B 361*, 1307-1315.

[33] Duff, M. R., Jr., Borreguero, J. M., Cuneo, M. J., Ramanathan, A., He, J., Kamath, G., Chennubhotla, S. C., Meilleur, F., Howell, E. E., Herwig, K. W., Myles, D. A. A., and Agarwal, P. K. (2018) Modulating Enzyme Activity by Altering Protein Dynamics with Solvent, *Biochemistry 57*, 4263-4275.

[34] Lee, J., Natarajan, M., Nashine, V. C., Socolich, M., Vo, T., Russ, W. P., Benkovic, S. J., and Ranganathan, R. (2008) Surface sites for engineering allosteric control in proteins, *Science 322*, 438-442.

[35] Appleman, J. R., Beard, W. A., Delcamp, T. J., Prendergast, N. J., Freisheim, J. H., and Blakley, R. L. (1990) Unusual transient- and steady-state kinetic behavior is predicted by

the kinetic scheme operational for recombinant human dihydrofolate reductase, *Journal of Biological Chemistry 265*, 2740-2748.

[36] Appleman, J. R., Beard, W. A., Delcamp, T. J., Prendergast, N. J., Freisheim, J. H., and Blakley, R. L. (1989) Atypical transient state kinetics of recombinant human dihydrofolate reductase produced by hysteretic behavior. Comparison with dihydrofolate reductases from other sources, *Journal of Biological Chemistry 264*, 2625-2633.

[37] Tuttle, L. M., Dyson, H. J., and Wright, P. E. (2014) Side Chain Conformational Averaging in Human Dihydrofolate Reductase, *Biochemistry 53*, 1134-1145.

[38] Dametto, M., Antoniou, D., and Schwartz, S. D. (2012) Barrier crossing in dihydrofolate reductase does not involve a rate-promoting vibration, *Molecular Physics 110*, 531-536.

[39] Masterson, J. E., and Schwartz, S. D. (2015) Evolution Alters the Enzymatic Reaction Coordinate of Dihydrofolate Reductase, *The Journal of Physical Chemistry B 119*, 989-996.

[40] Roston, D., Cheatum, C. M., and Kohen, A. (2012) Hydrogen Donor-Acceptor Fluctuations from Kinetic Isotope Effects: A Phenomenological Model, *Biochemistry 51*, 6860-6870.

[41] Singh, P., Abeysinghe, T., and Kohen, A. (2015) Linking Protein Motion to Enzyme Catalysis, *Molecules 20*, 1192.

[42] Kohen, A. (2015) Role of Dynamics in Enzyme Catalysis: Substantial versus Semantic Controversies, *Acc. Chem. Res. 48*, 466-473.

[43] Sikorski, R. S., Wang, L., Markham, K. A., Rajagopalan, P. T., Benkovic, S. J., and Kohen, A. (2004) Tunneling and coupled motion in the Escherichia coli dihydrofolate reductase catalysis, *J. Am. Chem. Soc. 126*, 4778-4779.

[44] Francis, K., Sapienza, P. J., Lee, A. L., and Kohen, A. (2016) The Effect of Protein Mass Modulation on Human Dihydrofolate Reductase, *Biochemistry 55*, 1100-1106.

[45] Kiefer, P. M., and Hynes, J. T. (2004) Kinetic Isotope Effects for Nonadiabatic Proton Transfer Reactions in a Polar Environment. 2. Comparison with an Electronically Diabatic Description, *The Journal of Physical Chemistry A 108*, 11809-11818.

[46] Singh, P., Islam, Z., and Kohen, A. (2016) Chapter Eleven - Examinations of the Chemical Step in Enzyme Catalysis, In *Method. Enzymol.* (Gregory, A. V., Ed.), pp 287-318, Academic Press.

[47] Stojković, V., Perissinotti, L. L., Willmer, D., Benkovic, S. J., and Kohen, A. (2012) Effects of the donor-acceptor distance and dynamics on hydride tunneling in the dihydrofolate reductase catalyzed reaction, *J. Am. Chem. Soc. 134*, 1738-1745.

[48] Warshel, A. (1984) Dynamics of enzymatic reactions, *Proc Natl Acad Sci U S A 81*, 444-448.

[49] Åqvist, J. (1993) Computer Modeling of Chemical Reactions in Enzymes and Solution, *J. Biochem. Biophys. Methods 26*, 241-243.

[50] Wang, L., Goodey, N. M., Benkovic, S. J., and Kohen, A. (2006) Coordinated effects of distal mutations on environmentally coupled tunneling in dihydrofolate reductase, *Proc. Natl. Acad. Sci. U.S.A. 103*, 15753-15758.

[51] Agarwal, P. K., Billeter, S. R., and Hammes-Schiffer, S. (2002) Nuclear Quantum Effects and Enzyme Dynamics in Dihydrofolate Reductase Catalysis, *J. Phys. Chem. B 106*, 3283-3293.

[52] Liu, C. T., Hanoian, P., French, J. B., Pringle, T. H., Hammes-Schiffer, S., and Benkovic, S. J. (2013) Functional significance of evolving protein sequence in dihydrofolate reductase from bacteria to humans, *Proceedings of the National Academy of Sciences 110*, 10159-10164.

[53] Wang, Z., Antoniou, D., Schwartz, S. D., and Schramm, V. L. (2016) Hydride Transfer in DHFR by Transition Path Sampling, Kinetic Isotope Effects, and Heavy Enzyme Studies, *Biochemistry 55*, 157-166.